Metal-Ligand Interactions and Salt Bridges as Sacrificial Bonds in Mussel Byssus-Derived Materials

Frédéric Byette,[†‡] Audrey Laventure,[†] Isabelle Marcotte,[‡] and Christian Pellerin*[†]*

[†]Département de Chimie, Université de Montréal, Montréal, Québec, H3C 3J7, Canada

[‡]Département de Chimie, Université du Québec à Montréal, Montréal, Québec, H3C 3P8, Canada

KEYWORDS: Byssus, Proteins, Biomimicry, Sacrificial bonds, Mechanical properties, Self-healing

ABSTRACT: The byssus that anchors mussels to solid surfaces is a protein-based material combining strength and toughness as well as a self-healing ability. These exceptional mechanical properties are explained in part by the presence of metal ions forming sacrificial bonds with amino acids. In this study, we show that the properties of hydrogel films prepared from a byssus

protein hydrolyzate (BPH) can also be improved following the biomimetic formation of sacrificial bonds. Strengthening and toughening of the materials are both observed when treating films with multivalent ions (Ca^{2+} or Fe^{3+}) or at the BPH isoelectric point (pI) as a result of the formation of metal-ligand bonds and salt bridges, respectively. These treatments also provide a self-healing behavior to the films during recovery time following a deformation. While pI and Ca^{2+} treatments have a similar but limited pH-dependent effect, the modulus, strength and toughness of films increase largely with Fe^{3+} concentration and reach much higher values. The affinity of Fe^{3+} with multiple amino acid ligands, as shown by vibrational spectroscopy, and the more covalent nature of this interaction can explain these observations. Thus, a judicious choice of treatments on polyampholyte protein-based materials enables to control their mechanical performance and self-healing behavior through the strategic exploitation of reversible sacrificial bonds.

INTRODUCTION

Biomimetic and bio-inspired materials are gaining increasing importance with the discovery and improved understanding of the outstanding structure and functions of biological materials. Recently, sacrificial bonds such as ionic bonds, hydrogen bonds, hydrophobic interactions, and metal-ligand coordination were revealed as structural elements that enhance the mechanical performances of some natural materials.[1-4] For example, the presence of metal ions in a protein matrix was shown to reinforce and/or to provide a self-healing capability to biological materials.[5, 6] These features were observed in particular with the byssus, a protein-based set of fibers tethering mussels to water-immersed solid surfaces.

The byssus threads are designed to protect mussels from the hostile coastal reef environment, e.g. the lift and drag forces of waves and tides. The mechanical properties of these fibers are governed by multiple factors including their heterogeneous protein content hierarchically assembled,[3, 7] the specific conformation of the various proteins,[8, 9] the pH of the surrounding media and the presence of metallic ions binding to amino acid ligands such as histidines and 3,4-dihydroxyphenylalanines (DOPA).[5, 10] During tensile deformation of individual byssus fibers, the sacrificial bonds in the histidine-rich regions of the byssus core can rupture before covalent bonds, thus preventing their critical failure. Therefore, these metal-ligand interactions both stiffen and toughen the byssal threads, providing an energy-saving and protective evolutionary strategy to mussels.[2, 11, 12]

The presence of metal-ligand sacrificial bonds in the byssus proteins, along with the elastic nature of the protein framework, was also shown to be responsible for the self-healing of the mechanical performance of the fibers, i.e., a partially recoverable hysteresis between the loading and unloading curves in cyclic uniaxial stretching experiments.[3,4,10] Once the initially applied stress is removed, the sacrificial bonds that were broken during deformation can reform and lead to a time-dependent partial recovery of the initial mechanical properties.[4] Some protein segments also contribute to an entropy-driven recovery by providing "hidden length" in the form of hydrogen bonded secondary structures that can deform or unfold reversibly under stress.[3, 10, 13, 14] The self-healing behavior procured by sacrificial bonds has recently led to the development of bio-inspired metallopolymers and synthetic peptides with tunable mechanical properties.[15-20]

In a previous study,[21] we demonstrated the possibility of preparing a byssus protein hydrolyzate (BPH) with good film forming ability. The BPH films are insoluble hydrogels as a result of the self-assembly of the polypeptides into collagen/gelatin triple-helices and β-sheets

that form strong physical crosslinks through multiple hydrogen bonding.[21] PPII helices, β-turns and unordered structures were also found within the BPH films and help provide extensibility to the protein network through their "hidden length". More importantly, and similarly to the native byssus[3, 13] and to elastin[22], the combined presence of reversibly unfoldable and aggregated structures can also lead to an entropy-related elastic recovery of the film after mechanical deformation. Interestingly, the BPH films were also shown to have pH-tunable mechanical properties because of their high content of charged amino acids (~30 mol %) that confers them polyampholyte-like properties. Films treated at their isoelectric point (pI) of 4.5 were stiffer and tougher because of attractive electrostatic interactions forming salt bridges acting like effective crosslinks. In contrast, acidic or alkaline pH generated electrostatic repulsion that led to a higher water swelling of the protein network and to mechanically weaker films.

In this study, we used a biomimetic approach to optimize the mechanical performance of the mussel-derived BPH films by inserting different metallic ions. We show that sacrificial bonds between amino acid ligands and the introduced cations allow tuning the stiffness and toughness of the BPH films as in the native byssus. We also observe the time-dependent self-healing behavior enabled by the salt bridges and metal-ligand sacrificial bonds in the BPH films.

MATERIALS AND METHODS

MATERIALS

Stocks of byssi were kindly provided by Moules de Culture des Îles Inc. (Magdalen Islands, QC, Canada) and MenuMer Ltée (Gaspé, QC, Canada). Byssal threads were first sorted to remove most of the unwanted sea products (algae, shells and other mollusk related parts) then thoroughly washed with soap under tap water. The cleansed product was rinsed several times

with distilled water and frozen at -20 °C. All other chemicals were of reagent grade and were used without further purification.

METHODS

Byssus protein hydrolyzate (BPH) preparation. The BPH was prepared as reported in our previous study.[21] Briefly, 5 g of cleansed and crushed dry byssi (predominantly the proximal and distal portions of the fibers since the plaques and columns were removed by a sieving procedure) were mixed in 150 mL of a 0.2 M KCl buffer system with 0.1 M sodium ethylene diamine tetra-acetate (EDTA) and adjusted to pH 13.5 with NaOH. The system was magnetically stirred at 4 °C for 7 days. The non-solubilized particles were removed by centrifugation and proteins from the supernatant were precipitated by adjusting the pH to 4.5 using acetic acid, and adding sodium chloride to reach a 0.5 M final concentration. The proteins were left to precipitate for 1 h before being pelleted by centrifugation at 5000 rpm at 4 °C for 20 min. The precipitate was dispersed in distilled water before being dialyzed (SpectraPor 3, MWCO 6-8 kDa, Spectrum Lab) for 3 days against distilled water. The precipitate was finally pelleted by centrifugation at 5000 rpm for 20 min at 4 °C before being freeze-dried. SDS-PAGE analysis[21] showed broad and intense bands between 50 and 60 kDa that correspond well with the apparent mass of pepsin-resistant α-like chains of Col-P (50 kDa), Col-D (60 kDa)[23] and Col-NG (60-64 kDa).[24]

Films preparation. The foam-like lyophilized BPH was crushed and dispersed in water before adjusting the pH to 10.5 using NaOH, reaching a final slurry concentration of 1 w/v %. The solution was pulse sonicated using a Microson XL-2000 ultrasonic homogenizer (Qsonica) for another 1 min. The solution was finally degassed by centrifugation for 2 min at 5000 rpm and

1 mL of the solution was poured into each well of a homemade Teflon mold (49 circular wells of 20 mm diameter). The solutions were left to evaporate in a fume hood until dry films were formed, usually for 96 h. The resulting water insoluble films were gently peeled off and washed with distilled water for 30 min before further treatments.

Metal treatment on BPH films. Hydrated pristine BPH films were immersed in 5 mL of 500 mM NaCl, $CaCl_2$ or $FeCl_3$ solutions for 2 h at room temperature. The films were then washed several times with distilled water to remove any free ions. Other films were first pre-treated at their pI (pH 4.5) for 2 h using 0.1 M citrate buffer, washed with distilled water, and finally treated with the above-mentioned metal ions solutions. Solutions with other concentrations of $FeCl_3$ were also used (i.e. 50, 5, 0.5 and 0.05 mM) to study the effect of iron content on the mechanical properties of the films. Finally, other films were first adjusted to pH 1 using a 0.5 M KCl buffer and then treated for 2 h in a 500 mM $CaCl_2$ solution (pre-adjusted to pH 1) to isolate the effect of pH on mechanical properties. For convenience, treatments using $FeCl_3$, $CaCl_2$ and NaCl will be referred to as Fe, Ca and Na, respectively, in the legend of the figures.

Mechanical testing. Static uniaxial stress-strain measurements were conducted on sections (10 mm x 5 mm) of the various films using an Instron 5465 mechanical testing frame equipped with a 50 N load cell and a BioPuls bath filled with distilled water at 37 °C. The films were mounted between the jaws and pre-conditioned in the water bath for ~2 min before applying a constant extension rate of 5 mm min^{-1}. The modulus was calculated using the initial linear portion of the curve, typically between 2 and 5 % strain.

Cyclic uniaxial tensile testing was performed using the same instrument with the BioPuls bath either filled with distilled water, 500 mM NaCl, 10 mM $NaHCO_3$ (pH 10.5) or 10 mM KCl (pH 1) buffer at 37 °C. To study the self-healing behavior of the mechanical performance, selected films were cycled between 0 and 35 % extension at 5 mm min^{-1} with different resting times between the cycles (0, 5, 20, 60 and 120 min). The modulus, stress at maximum strain and toughness values were extracted from the different experiments. To study the Mullins effect of the materials, films were stretched at a strain rate of 5 mm min^{-1} until a selected strain was reached. The stress was then relieved by returning to the initial strain (0 mm/mm) at the same rate of 5 mm min^{-1}. The strain was increased by 0.1 mm/mm for each cycle and the process repeated until failure.

Optical microscopy. Fluorescence optical microscopy images were acquired with a MicroPublisher 3.3 RTV camera (Qimaging) mounted on an Axioscope 2 microscope (Carl Zeiss Microscopy LLC) equipped for epifluorescence. The DAPI filter was used for excitation and emission of the blue fluorescence. The images were recorded using the same exposure time to enable comparison of the fluorescence intensity of the different materials. Bright field images were recorded in transmission mode using the same microscope.

Raman spectromicroscopy. Raman confocal spectromicroscopy was conducted using a LabRam HR800 (Horiba Scientific) with a 600 g mm^{-1} holographic grating. The spectra were acquired with 10-30 mW of a 785 nm diode laser focused on the sample through a 60X water immersion objective (NA 1.0). The slit opening was fixed at 500 μm while confocal hole was varied between 500 and 1000 μm depending on the signal intensity. A polynomial baseline was

applied to the spectra using LabSpec 6 spectroscopy suite (Horiba Scientific) in order to correct for the fluorescence signal.

Attenuated total reflection (ATR) Fourier transform infrared (FTIR) spectroscopy. Infrared spectra of the films were obtained using a Bruker Tensor 27 spectrometer with a liquid nitrogen-cooled mercury-cadmium-telluride detector and a Golden Gate diamond ATR accessory (Specac). Spectra were acquired by averaging 256 scans with a 4 cm^{-1} resolution. The spectra were first baseline corrected using the concave rubberband method in Bruker OPUS 6.0, then normalized with the standard normal variate method over the Amide II region (1580 to 1480 cm^{-1}) using LabSpec 6. Difference spectra in the Amide II region were also calculated using LabSpec 6.

RESULTS AND DISCUSSION

Effect of metal addition on tensile mechanical properties. We first explored the effect of Na^+, Ca^{2+} or Fe^{3+} addition on the tensile mechanical properties of the byssus protein hydrolyzate (BPH) films. These metal ions of different valence were chosen because of their natural abundance in the byssal threads.[25, 26] Figure 1a displays representative stress-strain curves for the pristine (i.e., without pH pre-treatment) BPH films with and without added metal ions. The results summarized in Table 1 show that the elastic modulus and ultimate tensile strength (UTS) increase in the presence of metal ions and with the valence of the ions. The addition of Na^+ increased the modulus and UTS by a factor of two while Ca^{2+} led to a ~3.5 times increase compared to the untreated pristine films. The addition of Fe^{3+} had a much larger effect, leading to a modulus ~15 times higher and to a sevenfold increase of UTS compared to the pristine films.

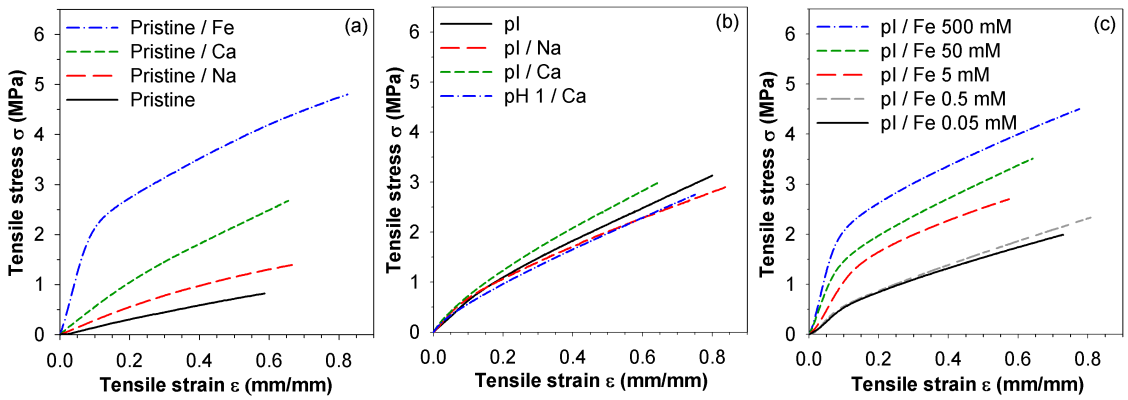

Figure 1. Representative uniaxial tensile stress-strain curves of (a) pristine (pH 10.5) byssus protein hydrolysate films without and with treatment with 500 mM NaCl, $CaCl_2$ or $FeCl_3$, (b) pI (pH 4.5) pre-treated films without and with further treatment in 500 mM NaCl or $CaCl_2$, and of pH 1 pre-treated films immersed in a 500 mM $CaCl_2$ solution, and (c) pI-treated films soaked in $FeCl_3$ solutions of 500, 50, 5, 0.5 and 0.05 mM.

The pristine films were formed at pH 10.5 where carboxylate functional groups are deprotonated and thus repulse one another, leading to a high water swelling ratio.[21] The presence of metal ions can screen these free electrostatic charges and create crosslinking points between aspartate and glutamate carboxylate groups, as well as other less abundant amino acids such as histidine, DOPA, asparagine and glutamine. They thus suppress the anionic repulsion, decrease the water swelling, and enhance the mechanical properties. As expected, Na^+ has the smallest impact on the mechanical performance of the pristine films since it cannot act as a crosslinker and only moderately screens charges. Even though the calcium binding with ligands is ionic, like for sodium, it can interact with more than one ligand and thus form effective crosslinking points. Iron can also bind with several ligands but it forms stronger complexes because of the more

covalent nature of the interaction, explaining the much larger impact of Fe^{3+} on the mechanical performance of the BPH films.

Table 1. Modulus, ultimate tensile strength (UTS) and strain at fracture (SF) of the different BPH films investigated (average ± standard deviation for N ≥ 5).

Film pre-conditioning	Metal addition (mM)	Modulus (MPa)	UTS (MPa)	SF (mm/mm)
Pristine (pH 10.5)	-	1.7 ± 0.5	0.7 ± 0.2	0.5 ± 0.1
	Na^{+} 500	3.3 ± 0.5	1.6 ± 0.4	0.7 ± 0.1
	Ca^{2+} 500	5.8 ± 0.5	2.7 ± 0.4	0.63 ± 0.07
	Fe^{3+} 500	28 ± 6	4.9 ± 0.6	0.8 ± 0.1
pI (pH 4.5)	-	9 ± 2	2.6 ± 0.5	0.7 ± 0.1
	Na^{+} 500	7 ± 2	3.0 ± 0.8	0.7 ± 0.2
	Ca^{2+} 500	8 ± 2	2.8 ± 0.6	0.7 ± 0.1
	Fe^{3+} 0.05	6.0 ± 0.9	2.1 ± 0.2	0.75 ± 0.09
	Fe^{3+} 0.5	8 ± 2	2.5 ± 0.5	0.7 ± 0.1
	Fe^{3+} 5	13 ± 2	2.4 ± 0.3	0.61 ± 0.09
	Fe^{3+} 50	18 ± 3	3.0 ± 0.7	0.6 ± 0.1
	Fe^{3+} 500	26 ± 7	4.5 ± 0.7	0.6 ± 0.1
KCl (pH 1.0)	Ca^{2+} 500	5.5 ± 0.6	2.4 ± 0.5	0.7 ± 0.1

We then studied the effect of metal ions on the mechanical performance of BPH films pre-treated at their pI using a citrate buffer (pH 4.5). BPH films were previously shown to have better mechanical performance at their pI as a result of salt bridges (interaction between carboxylate and ammonium functional groups) acting as effective crosslinking points in the protein matrix.[21] As seen from Figure 1b and Table 1, the addition of NaCl in pI-treated films slightly decreases the modulus compared to pI-treated films. These results support that NaCl

only affects the BPH films by screening the electrostatic charges within the protein matrix, thus enhancing the mechanical performances of the anionic pristine films but slightly diminishing those of the electrostatically crosslinked pI-treated films. Figure 1b also shows that $CaCl_2$ treatment has no notable effect on the mechanical properties of the pI-treated films when considering the standard deviation on the results. Therefore, the binding of Ca^{2+} with ligands only compensates for its screening effect over the favorable salt bridges interactions formed during pI treatment. This phenomenon will be further discussed below in the context of cyclic deformation experiments.

Figure 1c and Table 1 show the effect of $FeCl_3$ concentration on the mechanical properties of pI-treated BPH films. Treatment at the lowest concentration (0.05 mM) slightly decreases the elastic modulus and UTS compared to the control pI-treated film while treatment with the 0.5 mM $FeCl_3$ solution has no sizeable effect. The elastic modulus then strongly increases when the concentration of $FeCl_3$ is raised from 5 to 500 mM, reaching a value as high as that obtained for the pristine films treated with the 500 mM $FeCl_3$ solution. $FeCl_3$ solutions are acidic (500, 50, 5, 0.5 and 0.05 mM solutions have a pH of ~1.2, 2.0, 2.7, 3.3 and 3.9, respectively) and therefore reduce the pH of the protein matrix to some extent during the incubation. Thus, the addition of ferric chloride leads to three concomitant phenomena: 1) screening of the electrostatic charges within the protein network due to increased ionic strength, 2) metal-ligand bridging between amino acid moieties and 3) decrease of pH. The decreased modulus and UTS values for films treated with low Fe^{3+} concentration (i.e. 0.05 mM) is thus explained by charge screening and acidification of the protein matrix which disrupt the effective crosslinking provided by salt bridges and generate electrostatic repulsion, respectively. The modulus and UTS increase for

higher concentrations, in spite of the lower pH and higher ionic strength, due to the formation of effective iron-ligand crosslinking points, as will be demonstrated below.

Interestingly, none of the above treatments has a detrimental effect on the strain at fracture (SF, Table 1) of the BPH films and, as a consequence, their toughness increases. Indeed, metal ions can form sacrificial bonds in the protein matrix that have a lower strength than covalent bonds. When subjected to mechanical stress, these metal-ligand complexes can yield and dissipate the mechanical energy, thus sparing the covalent bonds from critical failure. This strategy exploited by mussels in the native byssal threads can thus be applied to mussel-derived BPH films to produce materials that are simultaneously stronger, stiffer and tougher.[2-4] However, since the preparation of the BPH films did not preserve the original protein integrity, the multi-level hierarchical assembly and the high orientation found in the native byssus, they remain mechanically weaker even following metal addition. Nevertheless, the elastic moduli of the BPH materials can be tuned over a range that corresponds well to that of soft biological tissues like skin, arterial walls, nerves and cartilage.[27]

Investigation of the metal-ligand interactions at the molecular scale. Different techniques were used to better understand the effect of metallic ions on the properties of BPH films and to validate the formation of sacrificial bonds. The BPH films have an intrinsic fluorescence which is mostly due to the presence of aromatic moieties, in particular DOPA residues.[26] Figure 2 shows that the fluorescence intensity varies with the type of metal ion used to treat the films and especially with the concentration of Fe^{3+}. The fluorescence intensity is similar for the pristine and pI-treated films with or without addition of Na^{+}. Similarly, Ca^{2+} only has a weak effect on the fluorescence (very low enhancement). In contrast, a gradual quenching of the fluorescence

occurs after incubation in $FeCl_3$ solutions of increasing concentration, which is a clear visual consequence of the formation of Fe-DOPA chelates. Indeed, it is known that paramagnetic metals like Fe^{3+} can strongly quench the fluorescence of some ligands via intramolecular energy transfer.[28]

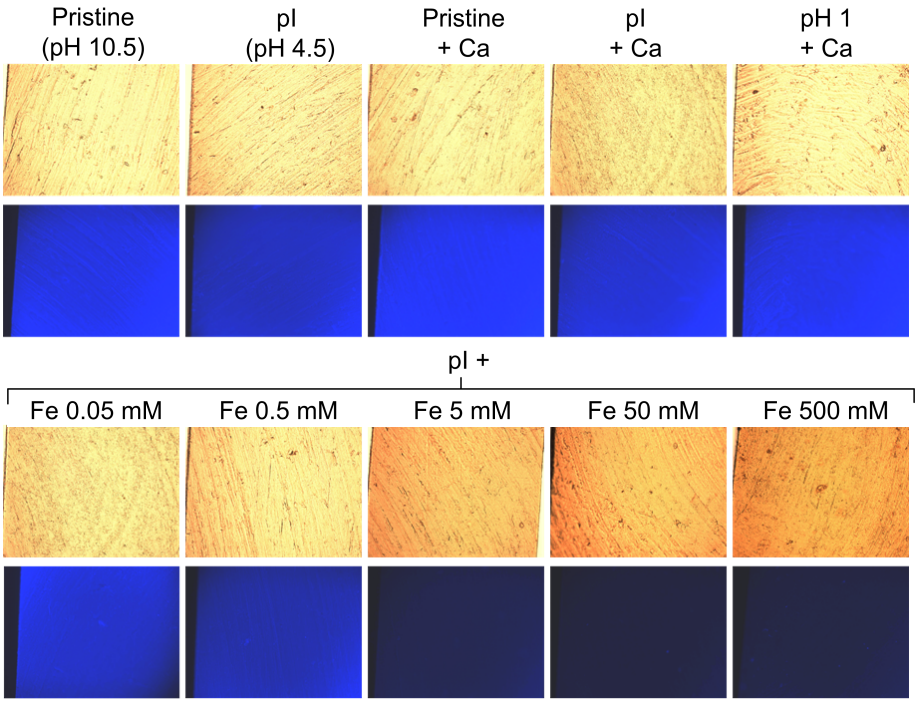

Figure 2. Optical and fluorescence microscopy images of BPH films treated in the conditions indicated.

Bright field optical microscopy images show no clear differences between most of the films. Only those treated with $FeCl_3$ concentration of 5 mM or more were darker as a consequence of Fe^{3+} ions sequestered in the protein matrix and/or of the formation of covalent di-DOPA crosslinks. In fact, the same phenomenon is observed in native byssal threads: fibers treated with citrate, a reducing and chelating agent, become golden-beige while those treated with iron are

dark-brown (data not shown). Two concomitant phenomena can lead to the observed darkening of the films. First, it can be ascribed to the formation of DOPA-Fe^{3+} complexes, which were reported to form within granules in the cuticule covering the fibrous core of the byssus and providing it with a hard but extensible protein-based coating.[5] Second, Fe^{3+} ions can oxidize the DOPA to generate quinones and semiquinone radicals that can further lead to di-DOPA covalent crosslinks.[29, 30] The propensity of DOPA to be oxidized increases at higher Fe^{3+} concentrations, during long exposure time and in the presence of oxygen, as seen in mussel adhesive proteins.[29, 31] Importantly, both the formation of di-DOPA and Fe-DOPA crosslinks can contribute to the increase in the mechanical performance of the iron-treated films seen in Figure 1 and Table 1.

Raman spectromicroscopy was used to investigate the presence of metal-ligand bonding sites within the BPH films. The Raman spectra of pI, sodium- and calcium-treated BPH films are practically identical and therefore do not provide much information on the interactions of these metal ions (data not shown). However, the spectra displayed in Figure 3a for films treated with $FeCl_3$ solutions show resonance-enhanced bands related to Fe-DOPA, DOPA and Fe-Histidine complexes. A broad band centered at 576 cm^{-1} with shoulders around 631 and 534 cm^{-1} indicates the formation of DOPA-Fe^{3+} complexes in the BPH films,[5, 17] with a similar overall spectral signature as previously reported for a Fe-DOPA-gelatin biopolymer.[32] These bands are absent for films treated at the lowest $FeCl_3$ concentration of 0.05 mM, small but clear for the 0.5 mM treatment, and prominent at higher concentrations. Bands characteristic of the catechol ring of DOPA also appear around 1266, 1320, 1427 and 1473 cm^{-1} in the spectra of films treated with Fe^{3+} at concentrations higher than 0.5 mM. These bands were also detected in the resonance Raman spectra of the cuticle of mytilids byssus fibers, in which tris-DOPA-Fe^{3+} complexes are formed as a strategy to enhance the mechanical properties of the threads.[5] Although Fe-DOPA

interactions are clearly detected in the Raman spectra and fluorescence microscopy images, the acidic pH environment in our experiments is believed to preferentially lead to the formation of mono or bis-DOPA coordination complexes. In particular, the broad peak shape in the low energy region of the Raman spectra (400-700 cm^{-1}) is highly similar that observed in the Raman spectra of synthetized PEG-$DOPA_4$ hydrogels treated with $FeCl_3$ in unadjusted pH conditions (pH ~3-4), while narrower bands were found after treatment at higher pH as a result of the formation of tris-DOPA complexes.[17] Considering that the mechanical performance of these synthetized hydrogels were enhanced by treatment at pH up to 12, it is possible that increasing the pH of our Fe-treated BPH films could also be a route to further enhance their mechanical performance. Finally, bands around 1565 and especially 1602 cm^{-1} increase in intensity relative to the amide I band for films treated with $FeCl_3$ solutions of 5 to 500 mM. Bands at similar positions were reported in the Raman spectra of synthesized histidine-rich mussel peptides, recombinant resilin peptides and other proteins,[4, 15, 20, 33, 34] making our results consistent with the formation of Fe-histidine interactions in the BPH films at high Fe^{3+} concentrations. However, this region of the Raman spectra strongly overlaps with the amide I band (1550-1750 cm^{-1}) as well as with signals from aromatic moieties found in the BPH like Phe, Tyr, Trp, and possibly DOPA, making a conclusive assignment to histidine-related bands difficult. Interestingly, the effect of iron bonding is only detectable in the Raman spectra for BPH films treated with a $FeCl_3$ concentration ≥0.5 mM, the lowest concentration leading to a strengthening effect (Table 1). This supports the conclusion that metal-ligand sacrificial bonds play a major role in the improvement of their mechanical properties.

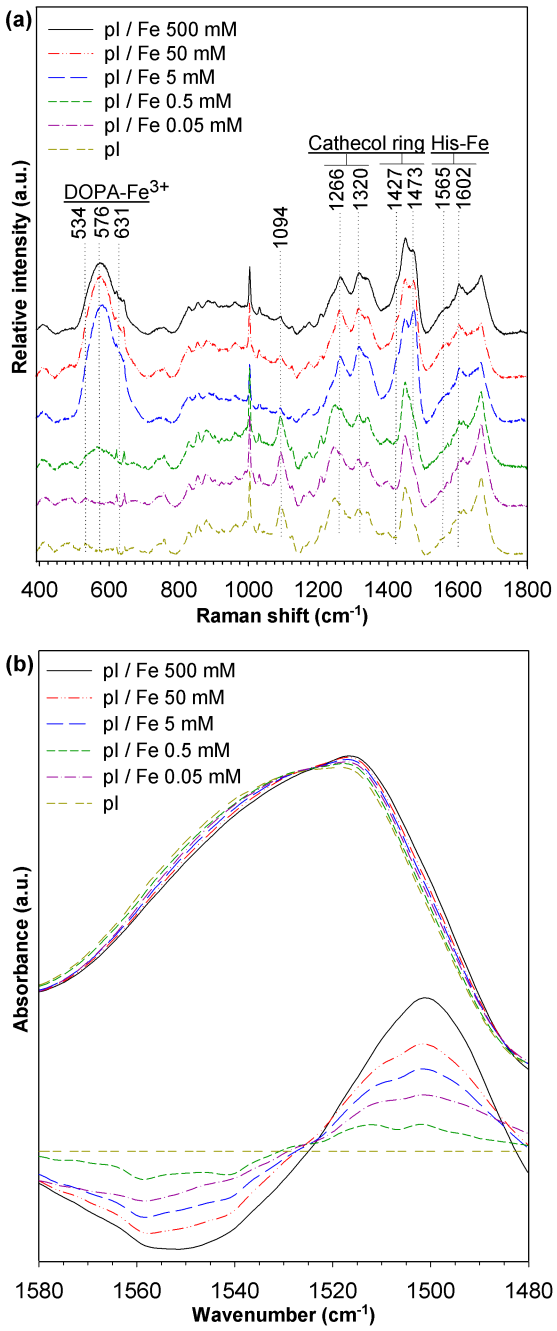

Figure 3. (a) Raman spectra of pI-treated BPH films incubated with $FeCl_3$ solutions of different concentrations and (b) FTIR spectra of the same films in the Amide II region (top) and their difference spectra relative to the pI-treated film (bottom).

FTIR spectra of proteins are dominated by the amide-related vibrations from the backbone and provide useful information on their secondary structure.[35, 36] Hence, infrared analysis was performed to monitor the effect of metal addition on the secondary structures within the BPH films. The FTIR spectra in the region from 1750 to 900 cm^{-1} are shown in Figure S1 of the Supporting Information. As previously found, analysis of the amide I band indicates a high content of aggregated strands and collagen structural elements.[21] Importantly, the spectra are very similar for all the materials studied, revealing that metal treatments did not affect the secondary structure of the BPH. This result indicates that the variation of the mechanical performance of the films is mostly related to the interactions of amino acid ligands with the incorporated metal ions, not to structural changes of the proteins. The formation of metal-ligand interactions can be detected as slight changes in band shape. Figure 3b shows the FTIR spectra and the difference spectra in the Amide II band range for pI-treated films incubated in solutions of various iron concentrations. An increased intensity of components around 1515 and 1500 cm^{-1} and a loss of intensity between 1580 and 1525 cm^{-1} is recorded with increasing $FeCl_3$ concentration. A component around 1515 cm^{-1} was previously reported for the protonated tyrosine side chain (Tyr-OH) while a component around 1500 cm^{-1} was assigned to its deprotonated state ($Tyr\text{-}O^-$).[37] Tyrosine being similar to DOPA (two hydroxyls for DOPA instead of one for Tyr), the enhancement of these bands in the spectra of $FeCl_3$ treated BPH films may be due to Fe-DOPA interactions, as observed more directly by Raman spectroscopy. Free carboxylate groups from aspartate and glutamate have infrared absorption bands around 1575 and 1560 cm^{-1}, respectively.[36] These bands may shift +60/-40 cm^{-1} upon cation chelation.[36] The loss of absorbance in this region could thus be linked to Fe-carboxylate interactions at higher Fe^{3+} concentration. Calcium treatment had much less effect on the FTIR spectra (Figure S2).

Even though these spectroscopy measurements do not provide quantitative information about the number and geometry of metal-ligand bonding sites, they clearly corroborate the propensity of Fe^{3+} to interact with DOPAs and suggest interactions with histidines and carboxylate groups in the BPH films. These results are in line with the improved mechanical performance (Table 1) provided by Fe^{3+} compared to Ca^{2+} and Na^{+}, for which no spectroscopic evidence of interaction was detected.

Mechanical performance and self-healing behavior under cyclic loads. Since functional biomaterials often undergo repetitive stress-induced deformation during their practical use, their ability to maintain or recover their mechanical properties must be investigated and optimized. As a biomimetic approach to byssus and to better understand the impact of metal ions, we investigated the mechanical properties of the BPH films under uniaxial tension cycles. Cycling the materials with strain increments and without recovery time between the cycles was first performed as shown in Figure S3 and described in the Supporting Information. Similar to the native byssal threads,[10] the BPH materials exhibited a viscoelastic behavior with a rubber-like Mullins softening effect.[38] However, since sacrificial bonds in the byssus are known to procure time-dependent self-healing of the mechanical properties, we investigated in detail the effect of recovery time on the materials properties.

Salt bridges as sacrificial bonds for the self-healing of BPH films. The pI-treated films were first cycled in a water bath or in a bath filled with a 500 mM NaCl solution to elucidate if salt bridges between charged amino acids can act as sacrificial bonds that procure a self-healing behavior to the byssus-derived materials. Representative curves in Figure 4 show the initial

deformation cycle, a second cycle without recovery (t = 0 min) and a cycle after a 120 min recovery time. In both distilled water and 500 mM NaCl baths, the samples stretched without recovery only possess ~60 % of their initial modulus and initial toughness, corresponding to the instantly recoverable elastic component. This 40 % loss can be explained in part by the presence of kinetically trapped domains formed during the protein self-assembly leading to the self-standing BPH films. These domains increase the stiffness of the initial films so that their stress-induced disruption and/or reorganization soften the materials. At the same time, the effective crosslinking points formed by salt bridges in the pI-treated films can also rupture under deformation and contribute to the softening observed when stretching the films without recovery (t = 0 min).

Figures 4 and 5 show that the initial loss of modulus and toughness can be partially recovered through a self-healing process when the pI-treated films are cycled in water. Their modulus and toughness gradually recover with resting time, reaching ~80 and 70 % of the initial values, respectively, after 120 min (Figures S8b and S9b in SI present the data expressed as percentages of the initial values). In contrast, the films cycled in the NaCl bath show essentially no recovery for the modulus (Figure 5a) and their toughness only recovers by ~5 % (Figure 5b) after 120 min of resting time. The main difference between these samples is the capability of the salt bridges to reform (in water) or not (in the NaCl bath) during recovery. When the salt bridges – acting as sacrificial bonds in the pI-treated films – collapse during stretching in the NaCl bath, Na^+ and Cl^- ions can interact with the freed negatively and positively charged amino acids, respectively. This screening prevents their reassembly and explains the absence or very limited recovery of modulus, toughness and strength (stress at maximum extension, see Table S1). Figure 5c shows that the mechanical work hysteresis decreases rapidly and then stays constant for the films cycled

in the NaCl bath because the softening effect is combined with a low permanent set (irrecoverable strain observed after retraction in Figure 4). On the other hand, the films cycled in water show a slower but gradual decrease of the work hysteresis because their increasing modulus is combined with a constant stress at maximum extension and a larger permanent set. The larger number of sacrificial bonds regenerated in the water bath provides a higher strength that opposes to the elastic restoring force of the protein network during retraction of the films, and thus leads to the larger permanent set observed in Figure 4 for films cycled in water.

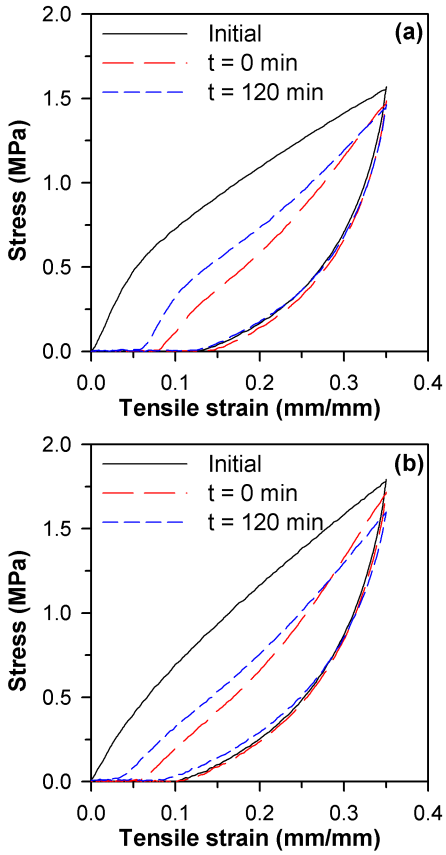

Figure 4. Representative cyclic tensile testing curves for the pI-treated BPH films stretched in (a) a water bath and (b) a bath containing 500 mM NaCl.

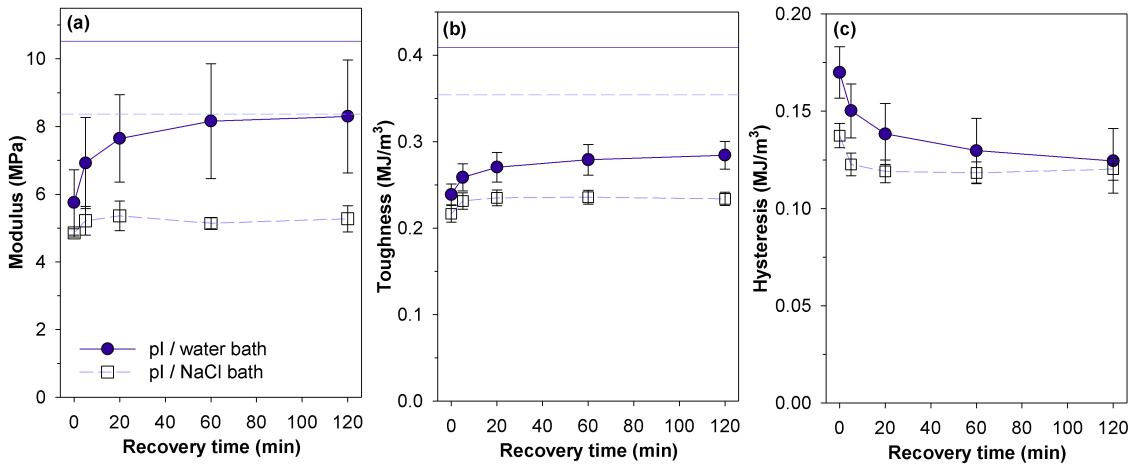

Figure 5. Modulus (a), toughness (b), and work hysteresis (c) of pI-treated BPH films measured during cyclic tensile deformation in distilled water or in a 500 mM NaCl solution. Values are reported for the initial stress-strain curves (reference horizontal lines) and for films allowed to recover (under no stress) for various times between the deformation cycles.

The results of Figures 4 and 5 confirm that the BPH films treated at their pI contain salt bridges that reinforce the films and act as sacrificial bonds during deformation. Their reassembly, most likely at new positions, during recovery in the water bath, but not in the NaCl solution, thus enable self-healing of the mechanical performance. This interpretation also explains the results for pristine BPH films cycled in distilled water or in a pH 10.5 bath (see Figures S4 and S5 in SI). These films should not contain a substantial amount of salt bridges due to the dominance of negatively charged amino acids. Cycling in distilled water leads to a gradual recovery of modulus and toughness, with the modulus even becoming larger than that of the initial sample after 120 min of recovery thanks to the formation of more salt bridges due to gradual shift of pH from 10.5 in the pristine film to closer to the BPH pI (4.5) upon cycling. In contrast, no recovery is observed in the pH 10.5 bath since salt bridges cannot form. Hence, the

regeneration of salt bridges or the creation of new ones is only possible in the absence of a high concentration of screening ions (water bath *vs*. NaCl bath) and if the pH of the surrounding solution is near the pI of the BPH. Interestingly, only films initially containing or forming new salt bridges as sacrificial bonds show a clear yield point in their representative stress-strain curves (see Figures 4a and S4a). A similar observation was reported for byssal threads treated with EDTA. Removal of ~50 % of the metal ions acting as sacrificial bonds in the native byssus led to the disappearance of the yield point and to the loss of its self-healing capability.[12]

Effect of Ca^{2+} at various pH. The addition of Ca^{2+} was found to have a negligible effect on the static mechanical properties of the pI-treated films (Table 1), which was explained by a competition between its bridging effect and the screening of salt bridges between charged amino acids. In contrast, the addition of Ca^{2+} to pristine films (pH 10.5) led to a large increase in modulus and to mechanical properties similar to those of films treated with calcium at pH 1 since there were essentially no salt bridges to be screened. Therefore, the effect of Ca^{2+} on the self-healing behavior of BPH films was studied at various pH. Pristine films (pH 10.5), pI-treated films (pH 4.5) and films pre-incubated at pH 1 were treated with a 500 mM $CaCl_2$ solution and their cyclic mechanical properties were studied at a pH equivalent to their pre-treatment. Figure 6 displays the modulus, toughness and cyclic work hysteresis after different recovery times (representative stress-strain curves are shown in Figure S6). The modulus and the toughness of the pI/calcium films highly recovered after 120 min of resting time (to ~90 and ~80 % of the initial values, respectively) and a yield point is clearly present in the representative stress-strain curves of Figure S6a. On the other hand, the pristine/calcium films had a much lower initial modulus which recovered less efficiently while their toughness remained almost fixed at ~70 %

of the initial value (the instantly recoverable part). Finally, films pre-treated at pH 1 and cycled in a bath at pH 1 had the lowest initial modulus and toughness and showed no recovery. This behavior highlights the distinct yet complementary effects of Ca^{2+} and salt bridges interactions as recoverable sacrificial bonds on the self-healing of the mechanical performance.

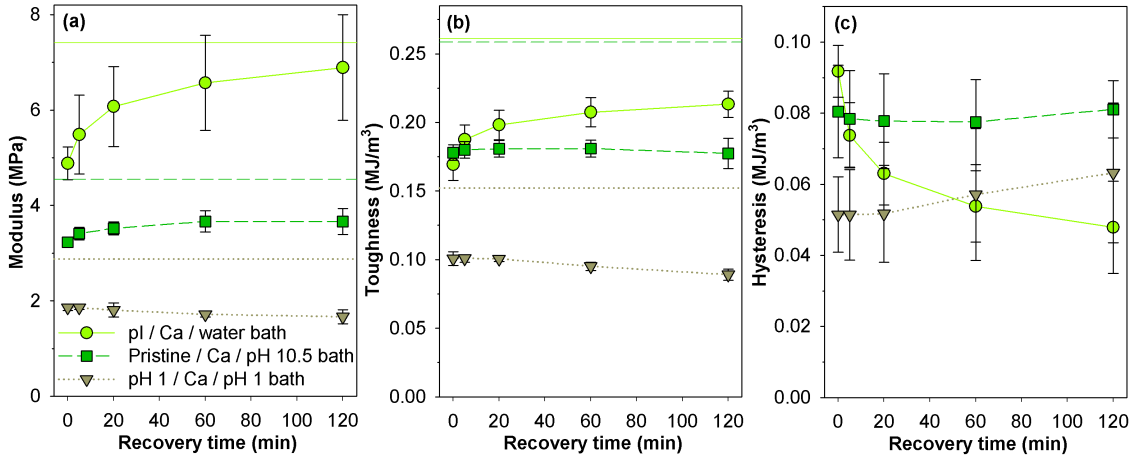

Figure 6. Modulus (a), toughness (b) and work hysteresis (c) values of BPH films pre-conditioned at three different pH (pI = 4.5, pristine = 10.5, and 1), further treated with 500 mM $CaCl_2$ and measured under cyclic tensile deformation in a bath at a pH similar to their pre-treatment. Values are reported for the initial stress-strain curves (reference horizontal lines) and for films allowed to recover (under no stress) for various times between the deformation cycles.

The self-healing behavior of the pI/calcium films cycled in water can further be observed in Figure 6c by their decreasing work hysteresis with recovery time. In contrast, the pristine/calcium films cycled at pH 10.5 maintained constant hysteresis values and the pH 1/calcium films showed a gradual softening upon cycling (increasing work hysteresis). These results can be attributed to the gradual regeneration of sacrificial bonds in the pI/calcium films

and to the release of calcium for the pH 1/calcium films, as reported at acidic pH (pH ≤ 3-5) for calcium-induced gelification of carboxylate-rich biopolymeric systems such as alginate[39] and soy proteins[40]. Similar results were observed on native byssal threads and histidine-rich mussel peptides treated at acidic pH,[10, 15] where the loss of mechanical performance and of the self-healing capability was associated to the protonation of histidines that hindered the metal-ligand interactions.

Calcium is able to bind to a large number of ligands with irregular and distorted geometries and the nature of the bonding is essentially ionic.[41, 42] It is thus assumed to form complexes that do not constrain the fluxional behavior of the protein network as much as a later transition metal would. The diffusion of calcium ions in the protein matrix might also contribute to a ligand exchange in order to attain the most favorable bonding configuration, as opposed to salt bridges that require reorganization of the protein network to form energetically optimized interactions. This can explain the propensity of calcium ions to increase the initial stiffness of the BPH films, but to only slightly affect the recovery. Forming sacrificial bonds using Ca^{2+} ions is an avenue to consider for controlling the mechanical properties of BPH films, but the pH of the environment must be carefully adjusted in order to reach the desired result.

Effect of Fe^{3+} concentration. Figure 7 shows the impact of Fe^{3+} ions on the self-healing behavior of pI-treated BPH films. As established in Figure 1 and Table 1, a greater concentration leads to much higher initial modulus and toughness in the representative cyclic curves of Figure S7. A yield point is clearly seen for all the conditions, in line with the strengthening effect of metal ions as sacrificial bonds reported for the native byssus.[10, 12, 13] Results summarized in Figure 7 show that the nominal values of modulus, toughness and work hysteresis at t = 0 min, i.e.

without recovery time after the first deformation cycle, increase with Fe^{3+} concentration, and that gradual recovery occurs with resting time for all concentrations. However, as highlighted in Figures S8d and S9d, the percentage of modulus and toughness recovered decreases with an increasing $FeCl_3$ concentration. Figure 7c and S9d also shows that a higher percentage of the work energy relative to the initial cycle can be retrieved between the cycles for the lower iron concentrations than for the higher concentrations. Nevertheless, it should be emphasized that all the Fe^{3+}-treated films retrieved 80 % or more of their initial modulus and 60 % or more of their initial toughness after 120 min of recovery (Figures S8d and S9d) such that their mechanical properties after cycling remain higher than those of films treated in other conditions. For instance, after 120 min of recovery, the modulus of $FeCl_3$-treated films ranges between 7 and 25 MPa, depending on the Fe^{3+} concentration, as compared to ~7 and ~8 MPa at best for pI/Ca and pI-treated films, respectively. This emphasizes the capability of Fe^{3+} to form sacrificial bonds that promote a concentration dependent self-healing capability and a high level of stiffening and toughening to the films.

The decreasing recovery relative to the initial films observed with increasing $FeCl_3$ concentration can be explained by the elastic protein network restoring forces and by the effect of Fe^{3+} concentration on the balance of sacrificial bonds between salt bridges and Fe-ligand complexes. Fluorescence microscopy, Raman and FTIR spectroscopy (Figures 2 and 3) showed no detectable Fe-ligand interactions at the lowest $FeCl_3$ concentration (0.05 mM) while Fe-DOPA and possibly other ligands were observed at higher concentration (≥0.5 mM). Salt bridges therefore dominate at low $FeCl_3$ concentration, making these films weaker than those with a higher Fe^{3+} concentration but improving their modulus and toughness recovery because of the easier diffusion of the polypeptides chains that are not constrained by Fe-ligand crosslinks.

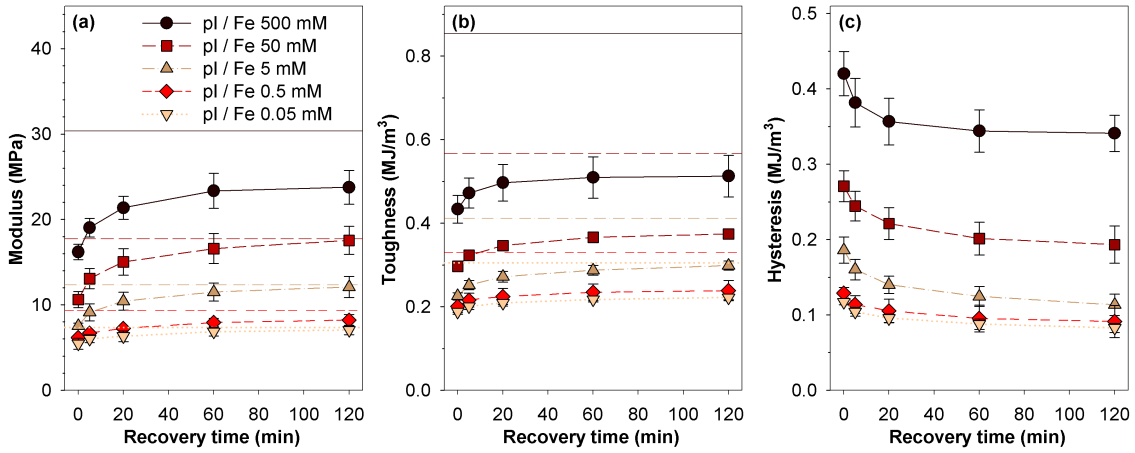

Figure 7. Modulus (a), toughness (b) and work hysteresis (c) values of pI pre-treated BPH films treated with various $FeCl_3$ concentrations and measured during the cyclic tensile deformation in a water bath. Values are reported for the initial stress-strain curves (reference horizontal lines) and for films allowed to recover (under no stress) for various times between the deformation cycles.

A recent study on the self-healing of the distal portion of native byssal threads suggested that the elastic protein framework would recover faster than the metal-ligand sacrificial bond could reform.[3] Following this rapid protein refolding, a ligand exchange between the various metal mediated sacrificial bonds was associated to the final step of the time-dependent self-healing.[4] This rearrangement of the Zn-histidines bonds would enable to reach a more stable state in the energy landscape of the byssus system.[4] Therefore, in our system, the fast initial recovery (t = 0 min) of the elastic protein framework and of the salt bridges would first bring the displaced amino acid ligands close to their original register, and then allow the reformation of the metal-ligand sacrificial bonds. When increasing the $FeCl_3$ concentration, the initial rapid rearrangement of the protein network would become hindered by the higher probability of forming Fe-ligand crosslinking points at new positions in the deformed protein network. These regenerated

sacrificial bonds would then act like kinetic traps and partially prevent the entropy-driven protein chain refolding responsible for the modulus recovery. This is in line with the observation of a greater permanent set for the films treated with a higher concentration of $FeCl_3$. Ultimately, as a biomimetic approach to native byssus, the formation of sacrificial bonds using iron increases the initial mechanical performances and provides a self-healing behavior to the BPH materials.

CONCLUSIONS

The bio-derived materials presented in this study retain some of the interesting features of native mussel byssus when subjected to a mechanical stress following the addition of metallic ions. Treatment of the byssus protein hydrolysate (BPH) films at their pI to create salt bridges and/or using multivalent metals found in byssal threads, i.e. Ca^{2+} and Fe^{3+}, was shown to create sacrificial bonds that increase the stiffness and strength of the materials without any detrimental effect on their extensibility, thus also increasing their toughness. A time-dependent self-healing behavior of the mechanical performances was found under cyclic uniaxial tensile testing. A treatment at the pI or the addition of Ca^{2+} to the films slightly enhanced their mechanical performance and recovery, but the addition of Fe^{3+} provided a much stronger effect that allowed to tune both the nominal values of the mechanical properties and their recovery rate. Spectroscopy experiments showed the existence of numerous Fe-ligand bonding sites, in contrast with Na^{+} and Ca^{2+}, which, along with their more covalent nature, help explain this higher strengthening effect. Overall, this study showed that BPH-based films have broadly tunable and self-healing mechanical properties following metallic ions addition in controlled conditions, a quality needed for applications involving repetitive stress or motions like in the field of biomechanics or prosthesis development.

ASSOCIATED CONTENT

Supporting Information. The following files are available free of charge. Additional FTIR spectra of films treated in various conditions; cyclic mechanical properties without recovery time; additional cyclic tensile testing curves and mechanical properties results; modulus and toughness recovery expressed as percentages of the initial values. (PDF)

AUTHOR INFORMATION

Corresponding Author

*E-mail: c.pellerin@umontreal.ca

*E-mail: marcotte.isabelle@uqam.ca

Author Contributions

The manuscript was written through contributions of all authors. All authors have given approval to the final version of the manuscript.

Notes

The authors declare no competing financial interest.

ACKNOWLEDGMENTS

This work was supported by a strategic research grant of the Natural Sciences and Engineering Research Council of Canada (NSERC) and funding from the Fonds de Recherche du Québec – Nature et Technologies (FRQNT). F.B. is grateful to the FRQNT for the award of scholarships. I.M. is a member of Ressources Aquatiques Québec (RAQ) and the Centre Québécois sur les

Matériaux Fonctionnels (CQMF). C.P. is a member of the Center for Self-Assembled Chemical Structures (CSACS).

REFERENCES

(1) Fantner, G. E.; Oroudjev, E.; Schitter, G.; Golde, L. S.; Thurner, P.; Finch, M. M.; Turner, P.; Gutsmann, T.; Morse, D. E.; Hansma, H.; Hansma, P. K., *Biophys. J.* **2006,** *90*, 1411-1418.

(2) Degtyar, E.; Harrington, M. J.; Politi, Y.; Fratzl, P., *Angew. Chem. Int. Ed.* **2014,** *53*, 12026-12044.

(3) Krauss, S.; Metzger, T. H.; Fratzl, P.; Harrington, M. J., *Biomacromolecules* **2013,** *14*, 1520-1528.

(4) Schmitt, C. N.; Politi, Y.; Reinecke, A.; Harrington, M. J., *Biomacromolecules* **2015,** *16*, 2852-2861.

(5) Harrington, M. J.; Masic, A.; Holten-Andersen, N.; Waite, J. H.; Fratzl, P., *Science* **2010,** *328*, 216-220.

(6) Waite, J. H.; Lichtenegger, H. C.; Stucky, G. D.; Hansma, P., *Biochemistry* **2004,** *43*, 7653-7662.

(7) Hassenkam, T.; Gutsmann, T.; Hansma, P.; Sagert, J.; Waite, J. H., *Biomacromolecules* **2004,** *5*, 1351-1355.

(8) Hagenau, A.; Papadopoulos, P.; Kremer, F.; Scheibel, T., *J. Struct. Biol.* **2011,** *175*, 339-347.

(9) Hagenau, A.; Scheidt, H. A.; Serpell, L.; Huster, D.; Scheibel, T., *Macromol. Biosci.* **2009,** *9*, 162-168.

(10) Harrington, M. J.; Waite, J. H., *J. Exp. Biol.* **2007,** *210*, 4307-4318.

(11) Lucas, J. M.; Vaccaro, E.; Waite, J. H., *J. Exp. Biol.* **2002,** *205*, 1807-1817.

(12) Vaccaro, E.; Waite, J. H., *Biomacromolecules* **2001,** *2*, 906-911.

(13) Harrington, M. J.; Gupta, H. S.; Fratzl, P.; Waite, J. H., *J. Struct. Biol.* **2009,** *167*, 47-54.

(14) Bertoldi, K.; Boyce, M., *J. Mat. Sci.* **2007,** *42*, 8943-8956.

(15) Schmidt, S.; Reinecke, A.; Wojcik, F.; Pussak, D.; Hartmann, L.; Harrington, M. J., *Biomacromolecules* **2014,** *15*, 1644-1652.

(16) Xu, Z., *Sci. Rep.* **2013,** *3*, 2914-2920.

(17) Holten-Andersen, N.; Harrington, M. J.; Birkedal, H.; Lee, B. P.; Messersmith, P. B.; Lee, K. Y.; Waite, J. H., *Proc. Natl. Acad. Sci. USA* **2011,** *108*, 2651-2655.

(18) Barrett, D. G.; Fullenkamp, D. E.; He, L.; Holten-Andersen, N.; Lee, K. Y. C.; Messersmith, P. B., *Adv. Funct. Mater.* **2013,** *23*, 1111-1119.

(19) Fullenkamp, D. E.; He, L.; Barrett, D. G.; Burghardt, W. R.; Messersmith, P. B., *Macromolecules* **2013,** *46*, 1167-1174.

(20) Degtyar, E.; Mlynarczyk, B.; Fratzl, P.; Harrington, M. J., *Polymer* **2015,** *69*, 255-263.

(21) Byette, F.; Pellerin, C.; Marcotte, I., *J. Mater. Chem. B* **2014,** *2*, 6378-6386.

(22) Tatham, A. S.; Shewry, P. R., *Trends Biochem. Sci.* **2000,** *25*, 567-71.

(23) Qin, X.; Waite, J. H., *J. Exp. Biol.* **1995,** *198*, 633-644.

(24) Qin, X.-X.; Waite, J. H., *Proc. Natl. Acad. Sci. U. S. A.* **1998,** *95*, 10517-10522.

(25) Seguin-Heine, M.-O.; Lachance, A.-A.; Genard, B.; Myrand, B.; Pellerin, C.; Marcotte, I.; Tremblay, R., *Aquaculture* **2014,** *426-427*, 189-196.

(26) Holten-Andersen, N.; Mates, T. E.; Toprak, M. S.; Stucky, G. D.; Zok, F. W.; Waite, J. H., *Langmuir* **2009,** *25*, 3323-3326.

(27) Vatankhah, E.; Semnani, D.; Prabhakaran, M. P.; Tadayon, M.; Razavi, S.; Ramakrishna, S., *Acta Biomater.* **2014,** *10*, 709-721.

(28) Waite, T. D.; Morel, F. M. M., *Anal. Chim. Acta* **1984,** *162*, 263-274.

(29) Sever, M. J.; Weisser, J. T.; Monahan, J.; Srinivasan, S.; Wilker, J. J., *Angew. Chem. Int. Ed.* **2004,** *43*, 448-450.

(30) Wilker, J. J., *Nat. Chem. Biol.* **2011,** *7*, 579-580.

(31) Wilker, J. J., *Curr. Opin. Chem. Biol.* **2010,** *14*, 276-283.

(32) Chan Choi, Y.; Choi, J. S.; Jung, Y. J.; Cho, Y. W., *J. Mater. Chem. B* **2014,** *2*, 201-209.

(33) Takeuchi, H., *Biopolymers* **2003,** *72*, 305-317.

(34) Reinecke, A.; Brezesinski, G.; Harrington, M. J., *Adv. Mater. Interf.* **2016**, DOI: 10.1002/admi.201600416.

(35) Jackson, M.; Mantsch, H. H., *Crit. Rev. Biochem. Mol. Biol.* **1995,** *30*, 95-120.

(36) Barth, A., *Biochim. Biophys. Acta* **2007,** *1767*, 1073-1101.

(37) Barth, A., *Prog. Biophys. Mol. Biol.* **2000,** *74*, 141-173.

(38) Diani, J.; Fayolle, B.; Gilormini, P., *Eur. Polym. J.* **2009,** *45*, 601-612.

(39) Draget, K. I.; Smidsrød, O.; Skjåk-Bræk, G., Alginates from Algae. In *Polysaccharides and polyamides in the food industry: properties, production, and patents*, Steinbüchel, A.; Rhee, S. K., Eds. Wiley-VCH Verlag GmbH & CO. KGaA: Weinheim, 2005; Vol. 1, p 30.

(40) Kroll, R. D., *Cereal Chem.* **1984,** *61*, 490-495.

(41) Harding, M. M.; Nowicki, M. W.; Walkinshaw, M. D., *Crystallogr. Rev.* **2010,** *16*, 247-302.

(42) Harding, M. M., *Acta Crystallogr., Sect. D: Biol. Crystallogr.* **2000,** *56*, 857-867.

Abstract graphic for:

Metal-Ligand Interactions and Salt Bridges as Sacrificial Bonds in Mussel Byssus-Derived Materials

Frédéric Byette,[†‡] Audrey Laventure,[†] Isabelle Marcotte,[‡] and Christian Pellerin*[†]*

[†]Département de Chimie, Université de Montréal, Montréal, Québec, H3C 3J7, Canada

[‡]Département de Chimie, Université du Québec à Montréal, Montréal, Québec, H3C 3P8, Canada